#331

# Production of the J(3.1) and $\psi'$(3.7) by 225 – GeV $\pi^+$, $\pi^-$ and Protons[*]

K.J. Anderson, G.G. Henry, K.T. McDonald[†]

C. Newman, J.E. Pilcher[‡], E.I. Rosenberg

Enrico Fermi Institute, University of Chicago,

Chicago, Illinois 60637

and

J.G. Branson, G.E. Hogan, R.D. Pisarski

G.H. Sanders, A.J.S. Smith, J.J. Thaler

Joseph Henry Laboratories, Princeton University

Princeton, New Jersey 08540

(Submitted to the XVIII Conf. in High-Energy Physics, Tbilisi, USSR, 1976.)

## ABSTRACT

We give preliminary results for J-production cross-sections in collisions of 225 GeV/c $\pi^+$, $\pi^-$, and protons with Carbon, and of 225 GeV/c $\pi^+$ and protons with Tin. (The J is observed in the decay mode $J \rightarrow \mu^+\mu^-$.) The total sample consists of 2100 J events. Differential cross-sections are given in terms of the variables $x_F = 2p^*_{//}/\sqrt{s}$, $p_\perp$, and $\cos \theta^*$, the polar angle of the $\mu$ in the J center of mass. We find the cross-section to increase linearly with atomic mass number of the target. The $\pi^+$ and $\pi^-$ - induced cross-sections are equal within the precision of the experiment. Pion-induced J's have a broader distribution in $x_F$ than proton-induced J's. The $p_\perp$-dependence seems to be independent of particle and target type. We find the average polarization of the J's to be consistent with zero for all beam and target types. Finally, estimates are given of $\psi'$(3.7) cross-sections.

# INTRODUCTION

In a recently concluded experiment at the Fermi National Accelerator Laboratory, we have measured the production of $\mu$-pairs in hadron-hadron collisions. The first results, a measurement of J production in 150-GeV/c $\pi^+$ and proton collisions with Beryllium, have been published[1], and reports on other aspects of the experiment have been contributed to this conference[2,3,4,5]. This paper presents preliminary results of a high-statistics measurement of $\mu$-pair production at 225 GeV, using beams of $\pi^+$, $\pi^-$, and protons, incident upon Carbon and Tin targets. The present discussion is confined to the mass region above 2 GeV, where the signal is dominated by the $J \rightarrow \mu\mu$ decay. There are also non-resonant pairs in this mass region, which are discussed in another contribution[4].

The detector, shown in Figure 1, has been described elsewhere[1], so only a brief outline of its properties will be given here. The essential feature is the large acceptance provided by the Chicago-Cyclotron Spectrometer (2.5 meter radius, 1.27 meter gap height). The spectrometer is sensitive to the entire forward hemisphere ($x_F \geq 0$) and has essentially uniform acceptance in $p_\perp$ out to $\approx 4$ GeV/c. Unique to this experiment is the wide coverage in the center of mass angle $\theta^*$ of the decaying $\mu$-pairs: significant sensitivity is maintained from $0 < |\cos\theta^*| \leq 0.8$.

The principles of the spectrometer operation are now discussed. Muons produced in interactions in the target are separated from the dominant hadron flux by a 2.2-meter thick iron absorber placed about 1.5 meters downstream from the target. We trigger only on interactions in the target (typically $\approx 0.25$ interaction lengths thick) by requiring at least 2 particles to hit the scintillation counter $T_4$. Three threshold gas Cerenkov counters along the

beam tagged pions and protons for each individual event. Typical beam fluxes and compositions were: for positive beam, $\approx 2 \times 10^6$ particles per 1 second burst, of which $\approx 16\%$ were $\pi^+$, the rest protons (Kaons and $\mu$'s were less than 1 or 2 percent); for negative beam, $\approx 5 \times 10^5$ $\pi^-$/burst.

For some of the running, multiwire proportional chambers upstream of the absorber and halfway through it were used to measure the muon directions before multiple Coulomb scattering in the absorber could deteriorate the resolution. However, these chambers were not used in the analysis reported here, the extra resolution being important mainly at lower masses.[2] For the analysis reported here, the muon directions were measured in front of the magnet by 8 planes (4X, 4Y) of MWPC between the absorber and the magnet.

Twenty planes of spark chambers measured the trajectories after they had passed through the magnet. Finally, the muons had to penetrate an additional 2.5 meters of iron and hit a large scintillator-hodoscope (shown as P in the figure). To suppress triggers from a single muon accompanied by a low-energy electromagnetic shower, we placed 8" of lead just in front of the P hodoscope and required at least two hits in <u>non-adjacent</u> scintillators. In much of the experiment, an additional suppression of low mass pairs was accomplished with a hodoscope (shown as J in the figure) consisting of two planes (X and Y) of ~4·cm·wide counters covering the acceptance of the MWPC's. We required at least two non-adjacent hits in either or both of the planes, thereby suppressing the trigger rate by a factor of 2 to 3 with negligible loss of pairs with masses above 1.5 GeV, even at the highest values of $x_F$.

The raw data for $M_{\mu\mu}$ > 2 GeV are shown in Figure 2. The widths of the J(3.1) peaks show our resolution. Part a) shows all p-induced events, part b) all $\pi^{\pm}$-induced events. In the inserts the scale is expanded for $M_{\mu\mu} \geq 3.35$ GeV, and in part c) of the figure all events from $\pi^{\pm}$ and p with masses $M_{\mu\mu}$ > 3.35 GeV

have been combined.  An apparent enhancement appears in all cases at M = 3.7 GeV,
which will be discussed later.  The continuum is discussed elsewhere.[4]

 To obtain differential cross-sections, the events in the mass range
$2.7 < M_{\mu\mu} < 3.5$ GeV were binned in $x_F$, $p_\perp$, and $\cos\theta^*$, and then corrected for
the spectrometer acceptance.  This efficiency was calculated by a Monte Carlo
simulation, which included effects of energy loss, multiple scattering and
bremsstrahlung, as well as the transport of the particles through the spectro-
meter to the final hodoscope.  To obtain absolute cross-sections we divided by
the effective luminosity, corrected for absorption of the beam in the somewhat
thick targets.  We collected approximately half of the positive-beam Carbon
data with a 7.46 cm thick target, the other half with a 12.54 cm target.  No
evidence, either in absolute rate or in energy distribution of the events, was
seen of secondary production, so we have combined the data from the two targets
in what follows.

 The differential cross-sections are shown in Figure 3 as a function of $x_F$,
in Figure 4 as a function of $p_\perp^2$, and in Figure 5, of $\cos\theta^*$.  The cross-sections
are expressed as nanobarns/nucleon, using a linear dependence upon the atomic mass
number A.  Comparing the data from Tin and Carbon targets, one sees that an
$A^{1.0}$ dependence is adequate, as observed by Binkley et al.[6] in neutron-nucleus
interactions.  A quantitative statement for the A-dependence of total cross-
sections is given below.

 The $x_F$-dependence of the cross-sections is, qualitatively, independent of
target type, and much broader for $\pi$-induced events than for those induced by
protons.  The data have been fitted to the form $\frac{d\sigma}{dx_F} = A(1-x)^b$, as suggested by
parton models; the results of the fitting procedure are given in Table Ia.  The
fit to the $\pi^-$-C data is not good, being dominated by one high bin, but aside
from that, the fits give a reasonable description.  The values for $\pi^+$ and p
induced events are in good agreement with earlier results[1,2] at 150 GeV/c .

Next, the distributions in $p_\perp^2$ were fitted to linear and quadratic forms, respectively:

$$B(J \to \mu\mu) \cdot \frac{d\sigma}{dp_\perp^2} = Ce^{-dp_\perp} \quad \text{and} \quad B(J \to \mu\mu) \cdot \frac{d\sigma}{dp_\perp^2} = Fe^{-gp_\perp^2} \quad .$$

As seen from the table, either parametrization is adequate, and there are no striking differences among the various reactions.

In table 1c are given the results of fitting the relative distributions in $\cos\theta^*$ of Figure 5 to the form

$$\frac{d\sigma}{d(\cos\theta^*)} = A(1 + \alpha\cos^2\theta^*) \quad .$$

In no case is there compelling evidence of any significant polarization of the J.

To find more precise values of $\alpha$, we have therefore combined all proton data (Figure 5f) and all $\pi^\pm$ data (Figure 5g), obtaining $\alpha_p = -0.26 \pm 0.19$ and $\alpha_\pi = 0.26 \pm .25$, respectively. Further study is required to see if the small polarization in the proton events is significant.

Values of the total cross-sections (times branching ratio) for J production are given in table II, for the range $0 \leq x_F \leq 1$. Two methods of obtaining them were used: first, we simply summed the values of $\frac{d\sigma}{dx_F}$ in Figure 3 over the $x_F$ bins, adding statistical errors in quadrature, and then doubling this error to allow conservatively for systematic effects. This method should be very reliable, because the spectrometer efficiency is insensitive to the $p_\perp$-dependence or $\cos\theta^*$ dependence of the cross-section. Second, to check the above method, we took the fitted functional forms $B \cdot \frac{d\sigma}{dp_\perp^2} = Fe^{-gp_\perp^2}$ and integrated over all values of $p_\perp$, getting $B \cdot \sigma = \frac{F}{g}$ . We have inflated the errors by a factor 1.5 somewhat arbitrarily, to account for the fact that the x-dependence of the data influences the absolute efficiency projected as a function of $p_\perp^2$. Good agreement between

the two methods is seen, so we conclude that the cross-sections of method 1 are accurately computed.

Several remarks can be made. 1) A-dependence. In obtaining the cross-sections per nucleon presented above, we have used a linear dependence on atomic mass number. To test this assumption, we now compare the actually measured total cross-sections per <u>nucleus</u> for Tin and Carbon targets. Assuming a power law $\sigma(A) \propto A^a$, we find:

$$\text{Proton Induced:} \quad \sigma(A) \propto A^{1.08 \pm .10}$$

$$\text{For } \pi^+ \text{ Induced:} \quad \sigma(A) \propto A^{1.03 \pm .15} \quad .$$

2) The ratio of the $\pi^+/\pi^-$ cross-sections for J production is consistent with unity:

$$\frac{\sigma^+(x>0)}{\sigma^-(x>0)} = 0.83 \pm .16 \quad .$$

In our final analysis, the error should be about half that given here, because in principle there are only very small systematic errors in this comparison.
3) The proton-induced cross-section is about half as large (for all x>0) as that for pion-induced events: averaging $\pi^+$ and $\pi^-$ results, we have, for Carbon,

$$\frac{\sigma_p(x>0)}{\sigma_\pi(x>0)} \simeq \frac{4.13 \pm .37}{8.97 \pm .92} = 0.46 \pm .063 \quad .$$

Again, this error will be reduced somewhat in the final analysis. 4) Dependence on beam energy: At 150 GeV, with a Be target, our final results[2] for the total cross-sections are

$$B \cdot \sigma_p(x_F>0) = 3.3 \pm 1.1 \quad \text{nb/nucleon}$$

$$B \cdot \sigma_\pi(x_F>0) = 6.5 \pm 2.2 \quad \text{nb/nucleon} \quad .$$

Thus, from $\sqrt{s} = 16.8$ ($E_{lab} = 150$ GeV) to $\sqrt{s} = 20.8$ ($E_{lab} = 225$ GeV), there is at most a very small increase in the cross-sections. This is consistent with

results of other experiments which measure $\left.\dfrac{d\sigma}{dy}\right|_0 \approx \dfrac{2M_J}{\sqrt{s}} \left.\dfrac{d\sigma}{dx}\right|_0$ for J production in proton-induced interactions at various energies. The quantity y is the center-of-mass rapidity. A sampling of these results[7] is shown in Figure 6, where $\dfrac{d\sigma}{dx}$ and $\dfrac{d\sigma}{dy}$ are plotted as a function of $\sqrt{s}$.

Looking back at Figure 2, we now discuss the production of the $\psi'(3700)$. To get as large a sample as possible we have combined Carbon and Tin data. Both for protons and pions, there is some indication of an enhancement at 3.7 GeV, although uncertainty in the subtraction of the continuum prevents a quantitative numerical measurement of $\sigma(\psi')$. Naively, we have attempted a subtraction assuming a straight-line continuum, obtaining 6 $\pi$-induced events, and 4 p-induced events. Using the same x- and $p_\perp$ dependences for $\psi'$ as for J, we can calculate the average detection efficiency and estimate roughly the ratio of $\psi(3700)$ to J production.

$$\text{Proton-Induced:} \qquad \frac{B\sigma(\psi'(3700))}{B\sigma(J)} \approx 3 \times 10^{-3}$$

$$\text{Pion-Induced:} \qquad \frac{B\sigma(\psi')}{B\sigma(J)} \approx 7 \times 10^{-3} \quad .$$

These values are lower than those reported by Snyder et. al.[7], who quote, at $y = 0$ (or $x_F = 0$), for protons on Beryllium,

$$\frac{B \frac{d\sigma}{dy}(\psi')}{B \frac{d\sigma}{dy}(J)} \approx 0.02 \quad .$$

Finally, in the mass range from 4 to 10 GeV, the average detection efficiency is $\gtrsim 12\%$. Only a few events are seen (Figure 1c), and there is no evidence for resonances to the level of this exposure, where 1 event $\lesssim 10^{-35}$ cm$^2$/nucleon.

## TABLE I. FITS OF J-PRODUCTION CROSS-SECTIONS

Note: To obtain cross-sections per nucleon, we have used a linear dependence on atomic mass number.

a) Dependence on $x_F$: $B \cdot \dfrac{d\sigma}{dx_F} = A(1-x)^b$ nanobarns/nucleon.

| Beam | Target | A | b | $\chi^2/dof$ |
|------|--------|-----|------|------|
| p | C | 22.3±1.8 | 3.98±0.20 | 3.6 |
| $\pi^+$ | C | 27.7±3.3 | 2.62±0.22 | 3.5 |
| $\pi^-$ | C | 39.1±5.0 | 2.15±0.16 | 5.2 |
| p | Sn | 25.8±3.4 | 3.94±0.30 | 4.1 |
| $\pi^+$ | Sn | 32.2±6.7 | 2.33±0.32 | 1.7 |

b) Dependence on $p_\perp$: (units of $\dfrac{d\sigma}{dp^2}$ are nanobarns/nucleon/$(GeV/c)^2$)

| Beam | Target | LINEAR $B \cdot d\sigma/dp_\perp^2 = Ce^{-dp_\perp}$ | | | QUADRATIC $B \cdot d\sigma/dp_\perp^2 = Fe^{-gp_\perp^2}$ | | |
|------|--------|-----|-----|------|-----|-----|------|
| | | C | d | $\chi^2/dof$ | F | g | $\chi^2/dof$ |
| p | C | 9.1±0.9 | 1.97±.08 | 1.8 | 3.5±0.3 | 0.80±0.06 | 1.2 |
| $\pi^+$ | C | 20.9±3.3 | 2.03±.15 | .5 | 7.9±1.2 | 0.88±0.12 | 1.6 |
| $\pi^-$ | C | 13.9±2.2 | 1.58±.13 | 1.5 | 6.2±0.8 | 0.59±0.06 | 1.0 |
| p | Sn | 9.8±1.5 | 1.86±.14 | 1.3 | 4.1±0.6 | 0.78±0.09 | 0.95 |
| $\pi^+$ | Sn | 13.2±4.5 | 1.56±.25 | 0.95 | 6.2±1.4 | 0.64±0.14 | 1.0 |

c) Dependence on $\cos\theta^*_{\mu\mu}$: we have fitted the form $d\sigma/d(\cos\theta^*) \propto (1+\alpha\cos^2\theta^*)$

| Beam | Target | $\alpha$ | $\chi^2/dof$ |
|------|--------|----------|------|
| p | C | −0.068±.24 | 3.14 |
| $\pi^+$ | C | 0.181±.37 | 0.64 |
| $\pi^-$ | C | 0.36 ±.44 | 1.3 |
| p | Sn | −0.947±.31 | 2.0 |
| $\pi^+$ | Sn | −0.35 ±.45 | 1.45 |
| p | C+Sn | −0.267±0.19 | 2.2 |
| $\pi^+,\pi^-$ | C+Sn | 0.26 ±.25 | 1.34 |

TABLE II.  TOTAL CROSS-SECTIONS FOR J PRODUCTION, 225 GeV BEAM

The best values are those of method 1 (see text).

| Beam | Target | No. of Events | $\sigma(x_F>0)$ Method 1 nb/nucleon | $\sigma(x_F>0)$ Method 2 nb/nucleon |
|------|--------|---------------|-------------------------------------|-------------------------------------|
| p | C | 868 | 4.13±0.37 | 4.37±0.50 |
| $\pi^+$ | C | 390 | 8.1 ±1.2 | 8.9 ±1.8 |
| $\pi^-$ | C | 350 | 9.8 ±1.4 | 10.5 ±1.7 |
| p | Sn | 331 | 4.85±0.7 | 5.3 ±1.0 |
| $\pi^+$ | Sn | 150 | 9.50±1.4 | 9.7 ±3.0 |

Note:  A linear dependence on atomic mass number has been used.

## REFERENCES

\* This research was supported in part by the National Science Foundation and by ERDA.

† Enrico Fermi post-doctoral fellow.

‡ A. P. Sloan fellow.

1. K.J. Anderson, et al., Phys. Rev. Letters $\underline{36}$, 237 (1976).

2. K.J. Anderson, et al., Inclusive μ-pair Production at 150 GeV by $\pi^{+}$ Mesons and Protons, submitted to the XVIII Conference on High-Energy Physics, Tbilisi, July 1976.

3. K.J. Anderson, et al., The Contribution of Muon Pairs to the Yield of Single Prompt Muons, Tbilisi Conference, 1976.

4. K.J. Anderson, et al., Continuum Muon Pairs Produced in Hadron-Hadron Collisions at 225 GeV, Tbilisi Conference, 1976.

5. K.J. Anderson, et al., High-Sensitivity Search for Multi-Muon Events Produced by 225 GeV Hadrons, Tbilisi Conference, 1976.

6. M. Binkley, et al., FNAL preprint 76/41-EXP, (1976).

7. J.J. Aubert, et al., Phys. Rev. Lett. $\underline{33}$, 1404 (1974); F.W. Büsser, et al., Physics Letters $\underline{56B}$, 482 (1975); Y.M. Antipov, et al., Physics Letters $\underline{60B}$, 309 (1976); H.D. Snyder, et al., Phys. Rev. Lett. $\underline{36}$, 1415 (1976).

## FIGURE CAPTIONS

Fig. 1     The Spectrometer.

Fig. 2     Mass distribution of $\mu$-pairs, uncorrected for apparatus efficiency.
a) proton-induced events, b) pion-induced events, ($\pi^+$ and $\pi^-$ samples
have been combined to give larger statistics), c) pion and proton
data combined, for masses above 3.35 GeV.

Fig. 3     Differential cross-sections $B(J\to\mu\mu)\cdot d\sigma/dx_F$ for J production. Fits
have been made to the form $(1-x)^b$.

Fig. 4     Differential cross-sections $B(J\to\mu\mu)\cdot d\sigma/dp_\perp^2$ for J production as a
function of $p_\perp^2$. The lines shown are fits to the form $Fe^{-gp_\perp^2}$.

Fig. 5     Relative differential cross-sections $d\sigma/d(\cos\theta^*)$ for J production.

Fig. 6     Energy dependence of J production cross-sections at $x_F = 0$. The
open points show $(d\sigma/dx_F)_0$, the solid points show $(d\sigma/dy)_0$, where y
is the center-of-mass rapidity. For experiments using nuclear
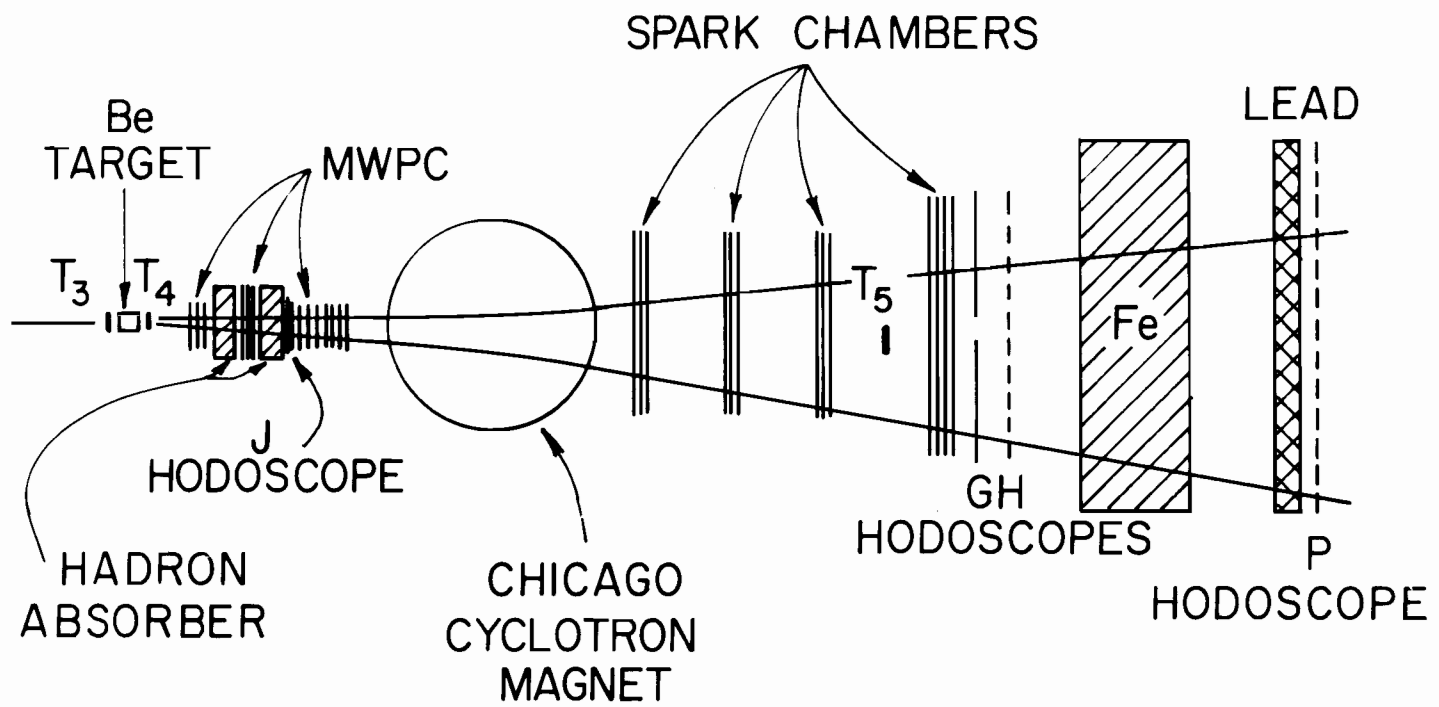targets, a linear A dependence has been used to obtain cross-
sections/nucleon.

FIGURE 1

a) $p + \binom{C}{Sn} \rightarrow \mu^+ \mu^- + X$

225 GeV

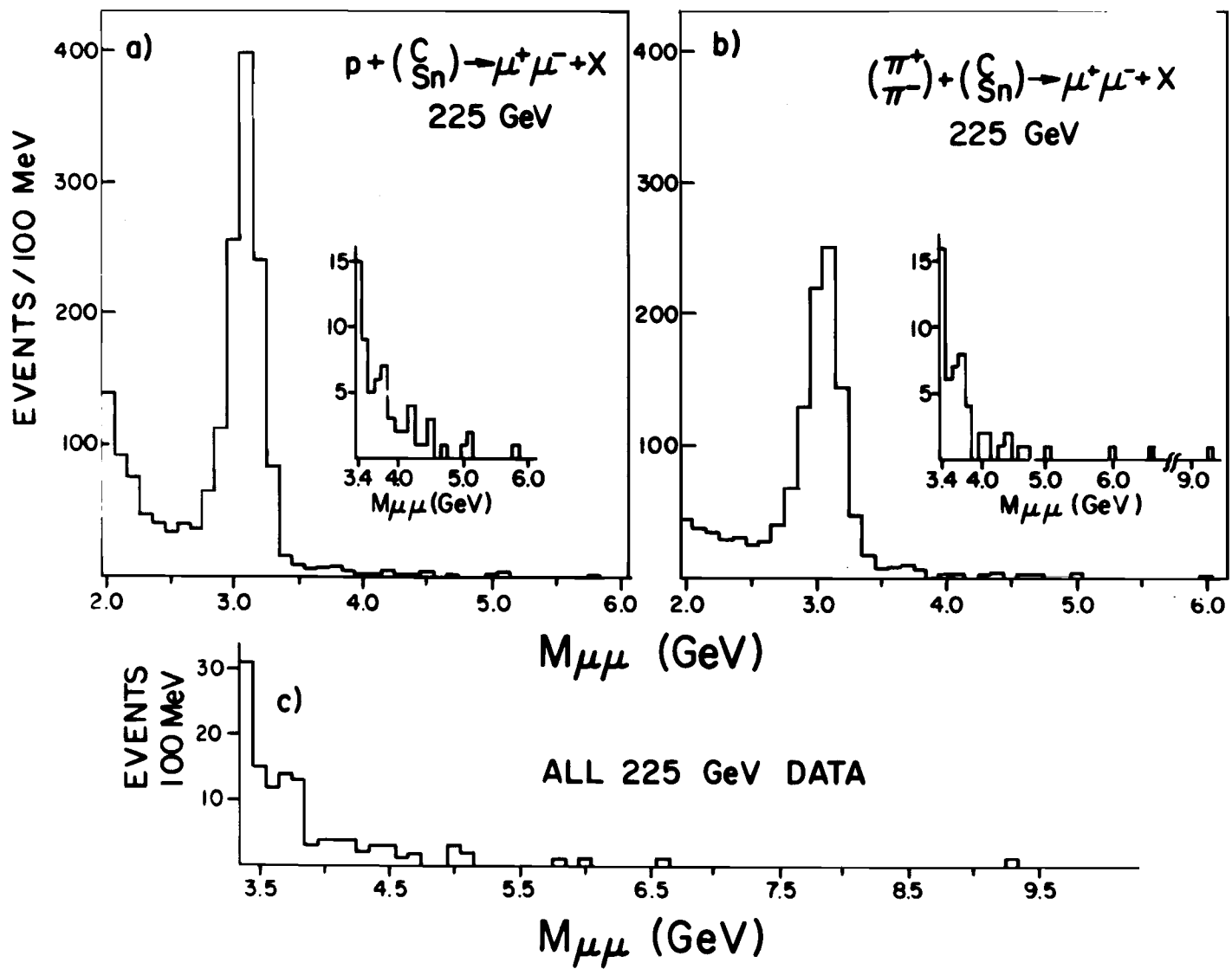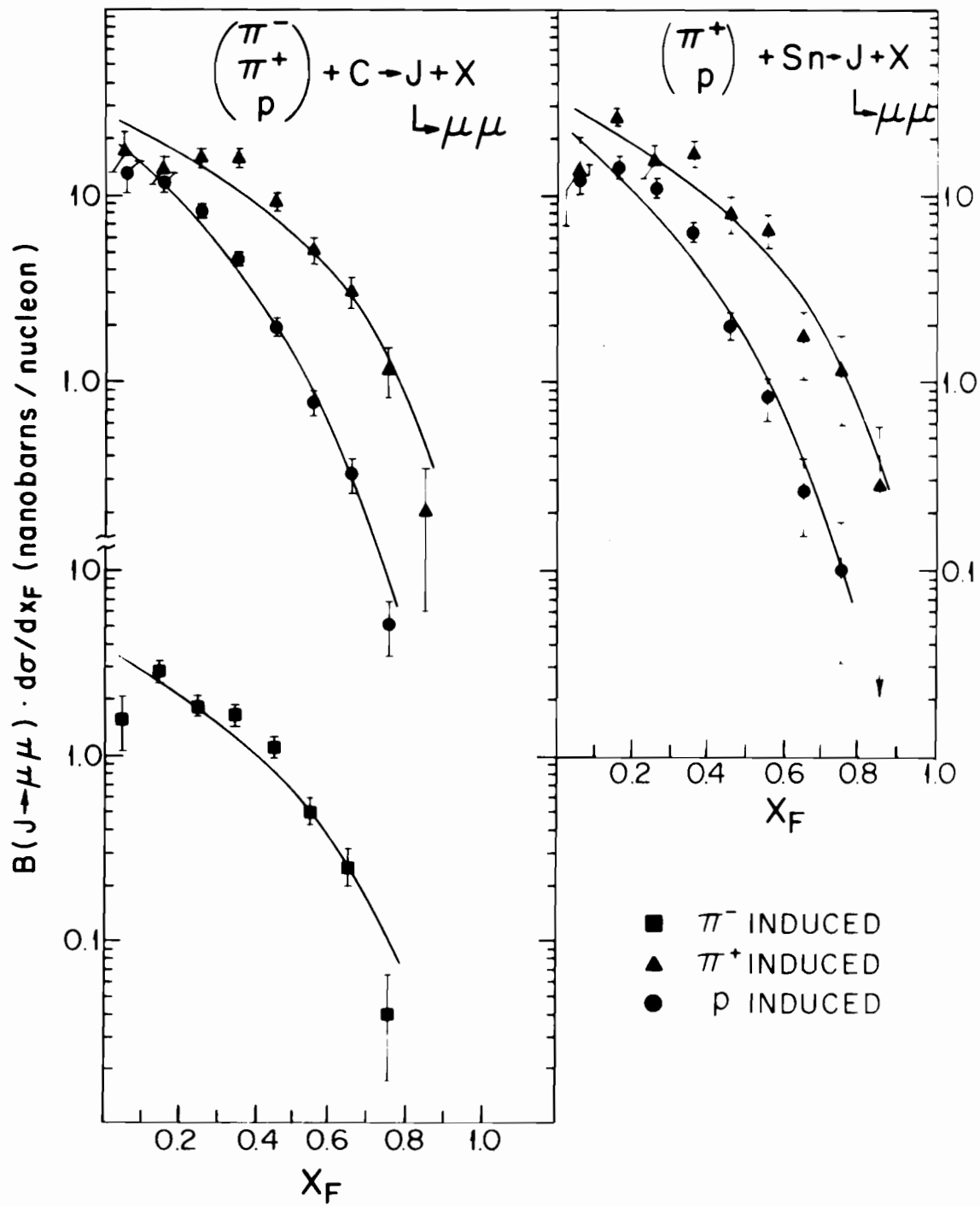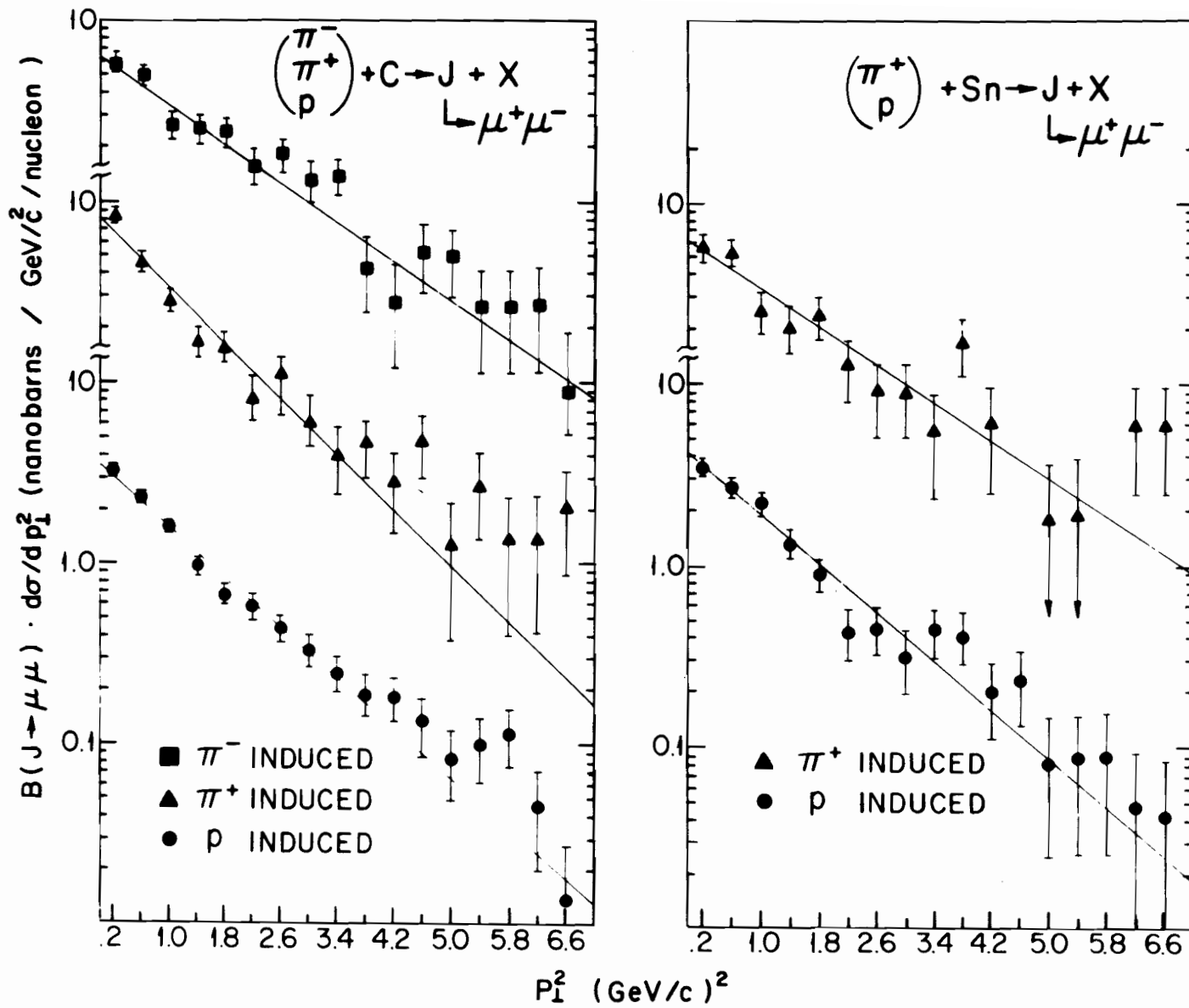b) $\binom{\pi^+}{\pi^-} + \binom{C}{Sn} \rightarrow \mu^+ \mu^- + X$
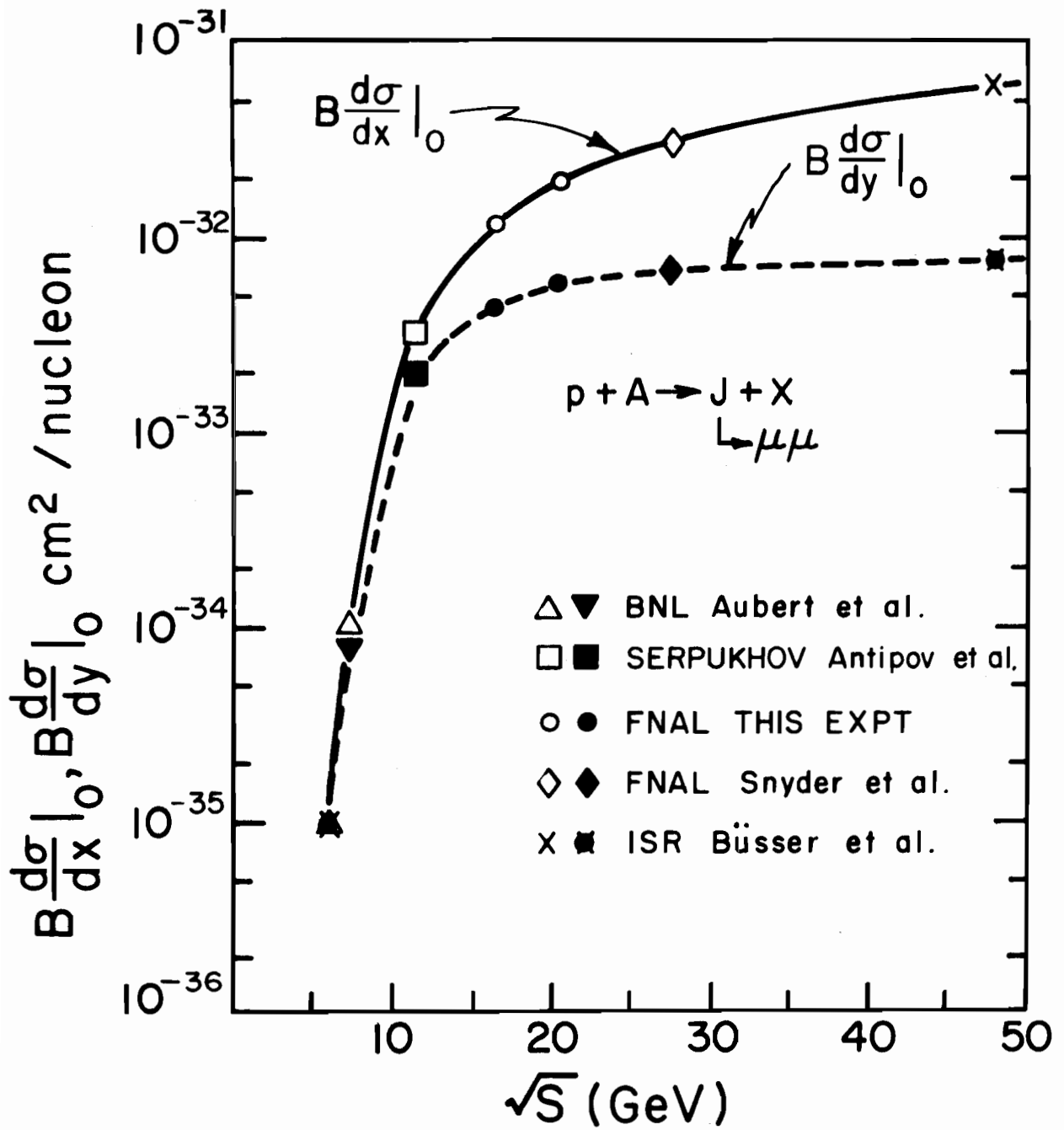
225 GeV

c) ALL 225 GeV DATA

FIGURE 2

FIGURE 3

FIGURE 4

FIGURE 5

FIGURE 6